

## The genesis of high magnesium andesites and basalts from Shodoshima in the Setouchi district, southwest Japan

\*Hidehisa Mashima<sup>1</sup>

1.Center for Obsidian and Lithic Studies, Meiji University

The genesis of high magnesium andesite (HMA) magmas in subduction zones is one of the most important issues of earth science. Results of high pressure melting experiments of peridotites demonstrated that two processes could form HMA magmas in the mantle, partial melting of hydrous peridotites at  $P \geq 1$  GPa and partial melting of anhydrous peridotites at  $P \leq 0.6$  GPa (Kushiro, 1969, 1972, 1974, 1996; Falloon et al., 1988; Hirose and Kawamoto, 1995; Hirose, 1997; Wood and Turner, 2009) .

The Setouchi HMAs distributed Shodoshima in SW Japan is considered to be formed by a reaction between slab-derived felsic melts and the mantle, a type of flux melting of peridotites (Shimoda et al., 1998; Tatsumi, 2006). The mantle/melt reaction model, however, has an insolvable petrological problem. Results of high pressure melting experiments indicate that the model requires additional processes forming a temperature difference larger than 150 °C in the mantle at a given pressure to explain the genetic relationships between HMAs and basalts coexisting in Shodoshima (Shimoda et al., 1998). The additional process has not been proposed by researchers advocating the mantle/melt reaction model.

In addition to this petrological incongruity, the mantle/melt reaction model is not consistent with seismic and geologic background of Shodoshima. The model considers that hydrous felsic melts would have been derived from sediments on the subducting Shikoku Basin lithosphere. The deep seismic zone representing the subducting slab, however, is not clear beneath Shodoshima, which implies that the subducting slab would not extend there even at the present day. The Setouchi magmatism occurred at around 14 Ma, which is the post period of the Takachiho Orogeny (20 -15 Ma). During the orogeny, the Shimanto accretional belt was uplifted (Sakai, 1990), which indicates a strong mechanical coupling between the SW Japan lithosphere and the Shikoku Basin lithosphere at that time. Under such a strong mechanical coupling between lithospheres, sediments on the Shikoku Basin would not have subducted effectively in the mantle. Instead, sediments would have been accreted to the SW Japan lithosphere. Sediments on the Shikoku Basin therefore would not have been transported beneath Shodoshima if the subducting slab reached there at that time. These seismic and geologic incongruities erode the confidence of the mantle/melt reaction model for the genesis of the Setouchi HMA magmas in Shodoshima.

Instead, these petrologic, seismic and geologic features indicate that the association of basalts and HMA in Shodoshima would have been formed by multi-stage partial melting of relatively anhydrous source mantle. The basalt magmas would have segregated at  $P > 1$  GPa and the HMA magmas would have finally segregated at  $P = 0.5$  GPa. In the context of the multi-stage partial melting model, geochemical features of the HMAs attributed to subducting sediments would be a result of involvements of accretional oceanic sediments at the base of the crust in the source mantle. This is consistent with results of an integrated seismic experiment across Setouchi implying forearc accretional belts such as the Sambagawa belt and/or the Shimanto belt would extend to the base of the crust beneath Shodoshima (Ito et al., 2009).

Keywords: high magnesium andesite, basalt, multi-stage partial melting

## Genesis of Quaternary volcanism of high-Mg andesitic rocks in the northeast Kamchatka Peninsula

\*Tatsuji Nishizawa<sup>1</sup>, Hitomi Nakamura<sup>1,2</sup>, Tatiana Churikova<sup>3</sup>, Boris Gordeychik<sup>4</sup>, Osamu Ishizuka<sup>5</sup>, Hikaru Iwamori<sup>1,2</sup>

1.Department of Earth and Planetary Sciences, Tokyo Institute of Technology, 2.Japan Agency for Marine-Earth Science and Technology, 3.Institute of Volcanology and Seismology, FED, RAS, 4.Institute of Experimental Mineralogy, RAS, 5.Geological Survey of Japan, AIST

Arc magmatism is a product of subduction factory, involving thermal and chemical interactions between a subducted slab as a material input and mantle wedge as a processing factory. In turn, the compositions of arc magma provide invaluable information concerning the material input and the interactions. The northeast Kamchatka Peninsula is an ideal field to examine such interactions and relationships, being characterized by (1) subduction of the Emperor Seamount Chain (Davaille and Lees, 2004), and (2) possible material and thermal interaction among the subducted slab, the overlying mantle wedge and the sub-slab mantle via the edge of subducted Pacific slab (Portnyagin and Manea, 2008). Within this area, a monogenetic volcanic group occurs along the east coast, including high-Mg andesitic rocks and relatively primitive basalts (East Cones, EC (Fedorenko, 1969)). We have conducted geochemical studies of the EC lavas, with bulk rock major and trace elements, and K-Ar and Ar-Ar ages, based on which a possible contribution of subducted seamounts and its relation to the tectonic setting are discussed.

The elemental compositions indicate that the lavas from individual cones have distinct mantle sources with different amounts and/or compositions of slab-derived fluids. Based on mass balance, water content and melting phase relations, we estimate the melting P-T conditions to be  $\sim 1200$  °C at 1.5 GPa, while the slab surface temperature is 620–730 °C (at 50–80 km depth). Compared with the southern part of Kamchatka, the slab surface temperature beneath EC seems to be high due to the thinner Pacific slab associated with the seamount chain and/or the plate rejuvenation from a mantle plume impact (Davaille and Lees, 2004; Manea and Manea, 2007).

The K-Ar and Ar-Ar ages of the Middle Pleistocene are consistent with the tephrochronological study (Uspensky and Shapiro, 1984) and the present tectonic setting after 2 Ma (Lander and Shapiro, 2007). The high-Mg andesite with the highest SiO<sub>2</sub> content in the EC lavas shows the oldest age ( $0.73 \pm 0.06$  Ma) within not only EC but also the northeast part of Kamchatka (e.g., Churikova et al., 2015, IAVCEI). On the other hand, the rest of EC lava samples show relatively younger ages to  $0.18 \pm 0.07$  Ma. These results suggest that the EC lavas including high-Mg andesite and basalt were generated by mantle flux-melting induced by dehydration of a subducted seamount inheriting a local thermal anomaly (Nishizawa et al., 2014, JpGU; 2015, JpGU).

Keywords: high-Mg andesite, island arc magma, Kamchatka arc, seamount subduction

Geology and petrology of Taisetsu volcano group, Japan; Evolution of magma and activity ages.

\*Kosuke Ishige<sup>1</sup>, Mitsuhiro Nakagawa<sup>1</sup>, Seiko Yamasaki<sup>2</sup>, Akikazu Matsumoto<sup>2</sup>

1.Earth and Planetary System Science Department of Natural History Sciences, Graduate School of Science, Hokkaido University, 2.GSJ, AIST

Taisetsu volcano group is located in the northern part of the Taisetsu-Tokachi volcanic chain, which is situated at the southern end of Kuril arc. The volcano group started its activity ca. 1 Ma and is composed of andesitic lava domes and stratovolcanoes.

Geological studies of the whole area in Taisetsu volcano group were carried out by Konoya *et.al.* (1966) and Katsui *et.al.* (1979). In these studies, the volcanic stratigraphy was investigated mainly based on the preservation state of the terrain, however, radiometric age data and petrological features were not considered. K-Ar ages reported in survey by NEDO (1990) are inconsistent with the stratigraphy, resulting in difficulty of re-examination of the stratigraphy. We performed a detailed geological survey, petrological study and K-Ar dating of the whole area of the volcano group, in order to investigate the structure of volcanic edifice, the formation history and the magma transition.

According to the preservation state of the terrain, petrological features and K-Ar ages of 26 samples, the activity of the volcano group can be divided into two stages; Older stage and Younger stage. During Older stage (ca. 1-0.7 Ma), fluidal andesite lavas were effused from several eruption centers to form flat-shaped volcanic edifices. These volcanic edifices are arranged in a N-S direction, and have been dissected by erosion. During Younger stage (< ca. 0.2 Ma), several stratovolcanoes and lava domes were formed in the northern - central part. Many of these volcanic edifices have the steep terrain, and are distributed irregularly. Younger stage is subdivided into three sub-stages (Y1, Y2 and Y3) in the difference of eruption style. In Y1 (0.16-0.06 Ma), stratovolcano and several lava domes were formed in the northwestern - central part. In Y2 (ca. 30 ka), the volcanic activities were the most explosive in the history. A plinian column and related pyroclastic flows were occurred, and formed the Ohachidaira caldera with 2 km in diameter. In Y3 (< ca. 30 ka), main eruption centers moved to the southwestern part of the caldera, and formed several stratovolcanoes and a lava dome.

K-Ar ages of the samples in Older and Younger stage are in the range of 1.02-0.66 Ma and 0.16-0.06 Ma, respectively. No ejecta are found between 0.66 Ma and 0.16 Ma, suggesting that there is a dormant period for ca. 0.5 Myrs in the history.

Petrological features of the ejecta of Taisetsu volcano group have greatly changed between the Older stage and Younger stage. All of the rocks are basaltic-andesite to dacite. These rocks contain Pl, Cpx, Opx and Mt as phenocrysts, associated with minor amounts of Ol, and Qz phenocrysts in some rocks. In addition, the rocks of Older stage do not contain Hb phenocrysts, while those of Younger stage usually include Hb phenocrysts. The host rocks from Older stage is characterized by high contents of incompatible element such as P<sub>2</sub>O<sub>5</sub>, Zr, Y, Nb, compared with those of Younger stage. The magma discharge step diagram of the volcano group was constructed based on the age data and estimated eruptive volume. The eruption rate of Older stage was >0.08 km<sup>3</sup>/ky, while Younger stage is >0.28 km<sup>3</sup>/ky. For Older stage, the eruption rate is maximized with 0.36 km<sup>3</sup>/ky in the period from 0.82 Ma to 0.74 Ma. For Younger stage, the eruption rate of each sub-stage is as follows; >0.20 km<sup>3</sup>/ky for Y1, >1.2 km<sup>3</sup>/ky for Y2, and >0.30 km<sup>3</sup>/ky for Y3. In addition, for the Y1, the eruption rate is the highest in 0.11 Ma to 0.09 Ma with 0.76 km<sup>3</sup>/ky.

Based on incompatible element contents and occurrence of Hb phenocryst in andesite, we consider

that magma type had changed largely during the possible long dormancy from 0.66 Ma to 0.16 Ma. This may be related to the tectonic change at the junction between NE Japan and Kuril arcs.

Keywords: Volcano, Eruption rate, Formation history, Transition of magma, Taisetsu volcano group

$^{14}\text{C}$  dating for the Holocene tephra deposits at the Esan volcanic complex, northern Japan

\*Daisuke MIURA<sup>1</sup>, Ken'ichi ARAI<sup>2</sup>, Ryuta FURUKAWA<sup>3</sup>, Michinori TAKADA<sup>4</sup>

1.Geosphere Sciences, Civil Engineering Research Laboratory, Central Research Institute of Electric Power Industry, 2.Asia Air Survey, Inc., 3.Research Institute of Earthquake and Volcano Geology, Geological Survey of Japan/AIST, 4.Department of Natural History Sciences, Graduate School of Science, Hokkaido University

Phreatic explosion is a smaller-sized eruption that is randomly generated from the pressurized steam chamber above a heat source. Thereby, the phreatic explosion may become hazardous, in the case where the social facilities or residential areas or people are very close to the active craters. Indeed, such a phreatic hazards has come arisen at the 2014 Ontake eruption, and then, it has widely become recognized as one of critical issues in volcanic hazards of Japan.

GSJ/AIST has a geological map project of "Esan Volcanic Complex (EVC)" since FY 2014. In the EVC, a large number of residential areas with tourist accommodations are located at the aprons where the distance to active fumarole craters is only 1-2 km. This spatial relationship implies a high risk of volcanic hazard even by a small phreatic explosion. Substantial information on the risk of phreatic explosions at EVC should be unraveled accurately. Yet, the spatial and temporal relationships of Holocene tephra deposits have been uncertain. We have therefore performed twelve measurements of  $^{14}\text{C}$  datings into the soils between Holocene tephra units.

The stratigraphic sequence of Holocene tephra units has been determined by the geological and geochronological studies, based on those originally established from Arai (1998 MS) (Okuno et al., 1999; CDPCEV, 2001; Miura et al., 2013). The sequence from the oldest to the youngest is EsMP, Es-1, Es-2, Es-3, Es-4, Es-5 and Es-6. EsMP is the episode of Esan lavadome (Ed) and block-and-ash flow (PDC) deposit, and is the largest in the Holocene eruption units. A charcoal in the PDC deposit has revealed the reliable  $^{14}\text{C}$  age of 8,648-8,594 cal yBP (1 sigma) for the EsMP. Es-1, 2, 3, 4, 5 and 6 are the unit originated from phreatic explosions at the Ed lavadome, and are constituted by phreatic ash-fall, pyroclastic surge (PDC) and/or lahar deposits. Previously obtained  $^{14}\text{C}$  ages (cal yBP) for these phreatic units are the followings. Es-1: 5,909-5,680 (bottom soil, 2 sigma), Es-3: 2,435-2,344 (a charcoal soil in PDC, 1 sigma), Es-4: 1,894-1,829 and 636-551 (bottom and cover soils, 1 sigma). Eruption ages of Es-5 (AD1846) and Es-6 (AD1874) have been determined by certain reliable documents.

Our new measurements of 12 samples (bottom and cover soils) for  $^{14}\text{C}$  dating have revealed a certain constraints into the eruptive ages of Holocene tephra units (cal yBP, 2 sigma). Es-1: 5,595-3,984, Es-2: 4,150-3,477, Es-3: 3,341-1,822 and Es-4: 681-536. These constrained ranges of eruption ages are consistent to the previously obtained  $^{14}\text{C}$  age results. The further constraint by all of available measurements implies that the Es-4 unit might have erupted at 681-551 cal yBP.

Keywords:  $^{14}\text{C}$  dating, phreatic explosion, Holocene, Esan volcanic complex

## The effect of external water to plinian and phreatoplinian eruption

\*Yoshimi Hiroi<sup>1</sup>, Tsuyoshi Miyamoto<sup>1</sup>

1.Center for Northeast Asian Studies, Tohoku University

Phreatoplinian eruption is one of phreatomagmatic eruption that occurs when vesiculated and fragmented felsic magma come into contact with external water. This eruptive style has not been observed yet, and it is defined by typical characteristics of deposits, which include enriched fine-grained ash particles produced by water cooling contraction granulation (Houghton et al., 2000) or phreatomagmatic explosion (Self and Sparks, 1978). Results of experiments on water-magma interaction (Hiroi and Miyamoto, 2012) and analyses of whole-grainsize distribution (Hiroi and Miyamoto, 2015) are contradictory to both fragmentation mechanisms, and therefore, this fine-grained feature must be the result of accretion by liquid water during transportation (Self and Sparks, 1978). Generally, the eruptive style is controlled by magma-water ratio, and magmatic eruptions occur when the amount of water is small enough than magma (Wohlets and Heiken, 1984). Koyaguchi and Woods (1996) simulated the behavior of an eruptive column affected by external water and showed that the column has been kept even if containing water account for 30wt%. Both plinian and phreatoplinian eruptions form eruptive columns; therefore, their borders appear to be dependent on the amount of water in the column. This study examines the effect of external water on plinian and phreatoplinian eruptions. The latest activity in Towada volcano is the Heian eruption, where the inner caldera lake in a double caldera was the vent, and all eruptions occurred through the lake water. Although the first unit OYU-1 erupted in contact with external water, it has been classified as a plinian eruption considering the features of the deposit such as facies, sorting, and F-D plot (Hiroi et al., 2015). OYU-1 contains cauliflower pumice (Heiken, 2006), which is rare although plinian eruptions are very common in the world. In addition, it does not exist in older plinian deposits in Towada volcano. The formation of cauliflower pumice requires an amount of water greater than that in the aquifer. However, the presence of cauliflower pumice implies that phreatoplinian eruptions do not occur unless external water is taken into the eruptive column even though magma come into contact with a large amount of external water. OYU-2 mainly consists of base-surge, and its characteristics such as fine-grained feature and vesiculated tuff correspond to phreatoplinian eruptions (Hiroi et al., 2015). The eruptive rate of OYU-2 is possibly larger than that of OYU-1. Although the water-magma ratio indicates magmatic eruption, OYU-2 is definitely a phreatoplinian eruption. The heat transfer efficiency from magma to water is expected to have increased because bubble growth in magma before contacting water increases successively from OYU-1 to OYU-2 (Hiroi and Miyamoto, 2011). Through heat transfer, steam is generated and the amount of water taken into the column is increased, effectively creating a wet column for phreatoplinian eruption. Plate-like glass shards indicating large expanded bubbles are outstanding in many phreatoplinian ejecta (Wohlets and Heiken, 1985). Cauliflower pumice did not form under quenching in phreatomagmatic activity, indicating that efficient heat transfer occurred. These suggest that bubble growth and heat transfer efficiency are very important for phreatoplinian eruptions to occur. With the abovementioned results, this study proposes that plinian eruptions affected by external water are common, because of non-existence both phreatomagmatic explosion and water cooling contraction granulation, the initial condition of phreatoplinian and plinian eruptions are the same, and phreatoplinian eruptions may occur if both the conditions of sufficient water and bubble growth are satisfied.

Keywords: phreatoplinian eruption, plinian eruption, Towada volcano, cauliflower pumice, heat transfer efficiency

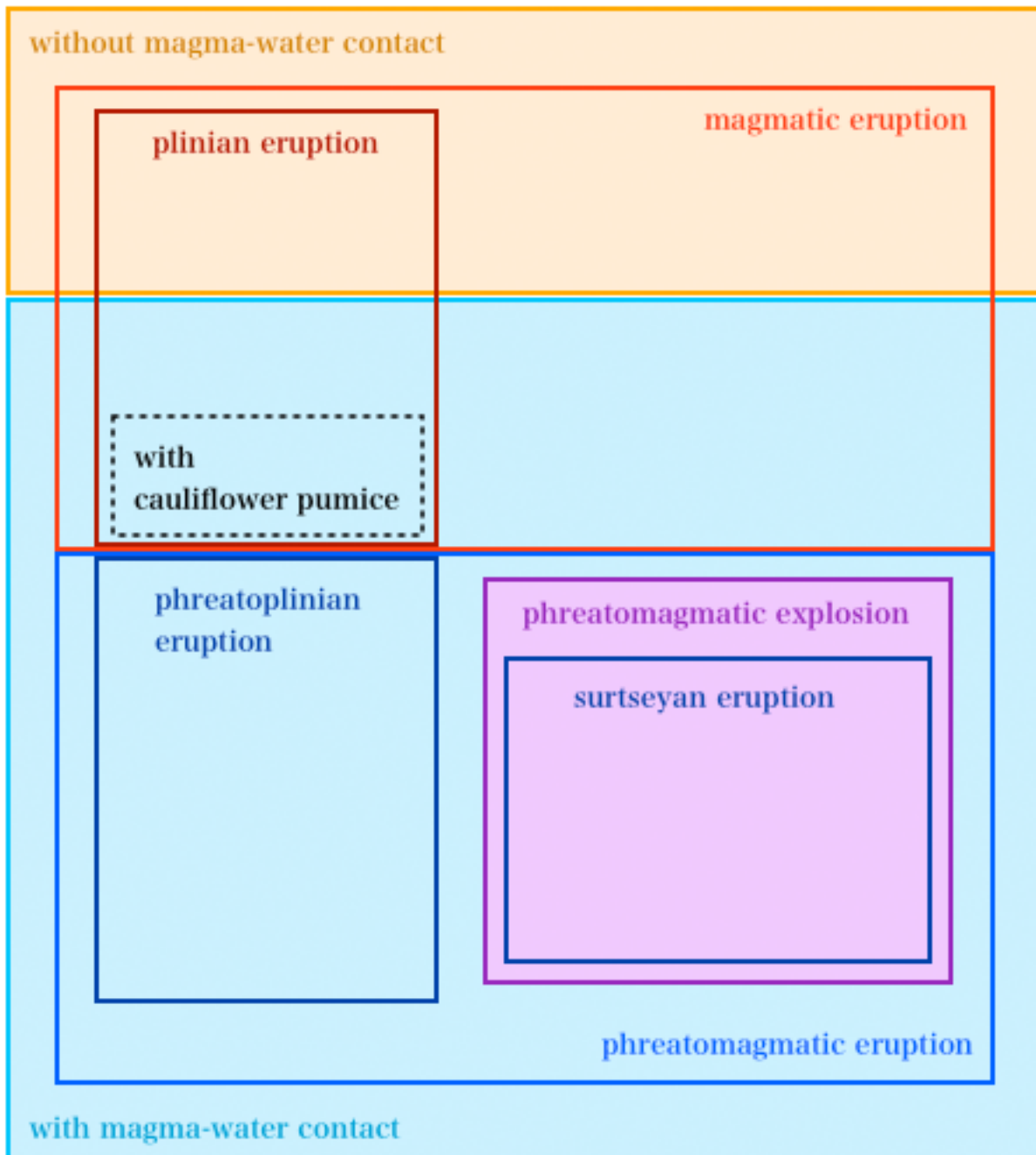


図. 本研究の結論から導かれる外来水の関与と噴火形態及び噴火様式の関係分類図

Fig. The new classification diagram of eruptive style on magma-water contact from this study.

## Geologic and petrologic study on basal part of the Goshikidake and adjacent lavas of the Zao volcano

\*Yuki Nishi<sup>1</sup>, Masao Ban<sup>2</sup>, Teruki Oikawa<sup>3</sup>, Seiko Yamasaki<sup>3</sup>

1. Graduate School of Department of Earth and Environmental Sciences, Yamagata, 2. Department of Earth and Environmental Science, Faculty of Science, Yamagata University, 3. Advanced Industrial Science and Technology

Zao volcano is an active stratovolcano in NE Japan, and has a long-eruption history of ca. 1 million years. Horse shoe shaped Umanose caldera was formed in the summit area at the beginning of the newest stage (ca. 35ka to present). The Goshikidake, the youngest cone, began to grow in the caldera at ca. 2ka. The present crater Okama is in the western part of the Goshikidake. We performed geologic and petrologic study on the basal part of the Goshikidake and adjacent lavas to reveal their magma feeding systems.

The Goshikidake is composed of Goshikidake pyroclastics, which is divided into 5 units. The lowest unit can be further divided into Goshikidake-nanbu pyroclastics, Goshikidake-toubu pyroclastics (pyroclastics main units). Near these pyroclastics, the Furikodaki lava and the Goshikidake-nanpo lava and pyroclastics (lavas main units) distribute. Goshikidake-nanbu pyroclastics are consisted of pyroclastic surge deposits and vent breccias. The latter intrude nearly vertically into the surge deposits. The Goshikidake-toho pyroclastics are composed of stratificated tuff ~ lapilli tuff ~ tuff breccia including various amounts of volcanic bombs. The Furikodaki lava flowed down from the northeastern base of the Goshikidake cone along a stream. The lava shows elongated shape with ca. 750m in length and 20~30m in width. The Goshikidake-nanpo lava and pyroclastics cropped out in a narrow area of ca. 650m south from the summit of Goshikidake. This unit is composed of upper brecciated lava with coarser lateral and finer vertical joints, and lower hyaloclastite-like tuff breccia.

All rocks are medium-K calc-alkaline olv bg. cpx-opx andesites (56-58wt% SiO<sub>2</sub>, 0.89-1.02 wt% K<sub>2</sub>O). Most of plagioclase phenocrysts has dissolution textures such as dusty zone and patchy zoning. We note that plagioclase phenocrysts in lavas main units lack the dusty zones.

The peak compositions of opx, cpx phenocryst core compositions are similar among units. These are 64-65 Mg# and around ca. 66 Mg#. The compositions of Mg-rich mantles of opx phenocrysts within ca. 30 um from rims are wider in rocks from the lavas main units than the pyroclastics main units. The core compositions of plagioclase phenocrysts show wide range of An<sub>62-92</sub>. The main peak compositions in the lavas main units are in An<sub>68-70</sub> and around An<sub>78</sub>, and subordinate peak is in An<sub>90</sub>. Those of the pyroclastics main units are in An<sub>64-66</sub>, An<sub>76-78</sub>, and An<sub>90</sub>. These petrologic features suggest the products were formed by magma mixing of mafic and felsic end-member magmas.

Bulk SiO<sub>2</sub> contents of the lavas main units are 57.5-58wt%, while those of the pyroclastics main units are 56-57.7wt%. As a whole, all products are plotted on same variation trends in silica variation diagrams, but looking at detail, rocks from the pyroclastics main units show higher trend in FeO, TiO<sub>2</sub>, Rb/Zr diagrams and lower trend in MgO diagram than the other products.

Although the bulk compositions are slightly different between the pyroclastics main and lavas main units, the bulk SiO<sub>2</sub>, phenocryst assemblage, and T-P-H<sub>2</sub>O conditions of the felsic end-member are similar for all units. These are estimated to be 62 wt% SiO<sub>2</sub>, Mg# 63-66 opx + Mg#65-70 cpx + An<sub>60-70</sub> plg, ca. 1000 °C, 1.7-2.7kb, 2.5wt% H<sub>2</sub>O, while those of mafic end-member are 48-49wt% SiO<sub>2</sub>, An<sub>90</sub> plg + olvine (Fo<sub>78</sub>), ca 1100 °C, <2kb, 2.0wt% H<sub>2</sub>O.

We calculated the time scales from magma mixing to the eruption by comparing the zoning profiles and calculated diffusion ones for olv, plagioclase, and opx phenocrysts. The obtained time scales



for olv, plagioclase, and opx are 1 year to 3 years, 80 to 300 days, and ~ 100 years. The percentage of longer lived opx is higher in the lavas main units.

Keywords: Zao volcano, Andestic lava, Pyroclastic surge, Magma mixing

## Stratigraphical study on the Middle Pleistocene pyroclastic flow deposits, northern Tochigi and southern Fukushima Prefectures and the eruptive history of Takahara volcano

\*Masataka Yamada<sup>1</sup>, Takayuki Kawai<sup>2</sup>, Haruka Saito<sup>1</sup>, Amao KASAHARA<sup>1</sup>, Fumikatsu NISHIZAWA<sup>1</sup>, Takehiko Suzuki<sup>1</sup>

1.Faculty of Urban Environmental Sciences, Tokyo Metropolitan University, 2.KOKUSAI KOGYO CO., LTD.

Introduction Middle Pleistocene pyroclastic flow deposits are distributed in northern Tochigi and southern Fukushima Prefectures. Shiobara-Otawara pyroclastic flow deposit (So-OT; Suzuki et al., 2004) is widely distributed in the northern Tochigi Prefecture. Moreover, fall-out tephra of So-OT is distributed into southern Aizu region (Suzuki et al., 2004), off Shimokita Core (Suzuki et al., 2012). However, there are controversy on stratigraphy and ages of So-OT and its related tephras. This is caused from the difference in the identifications of APms (Suzuki & Hayakawa, 1990) and KMT (Suzuki, 2000). This paper discusses the stratigraphy and ages of So-OT and its related tephras, and refers to the source of two newly defined tephras. Finally, we discuss the eruptive history of Takahara volcano.

Characteristic properties of the pyroclastic flow deposits We recognized three pyroclastic flow deposits, that is, So-OT, First Shiobara-katamata Tephra (So-KT1; new defined), and Second Shiobara-katamata Tephra (So-KT2; new defined) in descending order. So-OT is roughly divided into lower and upper parts. Lower part is a pumice fall deposit. Upper part is pyroclastic flow deposits. This pyroclastic flow deposits are divided into pumice flow deposit (lower), pumice flow deposit (middle), and scoria flow deposit (upper). Middle pumice flow deposit is widely distributed in the area from Utsunomiya City to Nasu Town, and is cropped out in the Yaita Hills as the thickest deposit. So-KT1 is divided into Unit a-d. Unit b is a pyroclastic flow deposit, and widely distributed in the east part of Yaita Hills. Refractive index of orthopyroxene in So-KT1 is higher than those in So-OT and So-KT2. Major chemical composition of volcanic glass shards of So-KT1 is distinguishable from those of So-OT and So-KT2. So-KT2 is a pumice flow deposit. The differences between So-KT1 and So-OT are mineral assemblage (only So-KT2 contains quartz and small amount of hornblende), and major chemical composition of volcanic glass shards.

Stratigraphy and ages of the pyroclastic flow deposits Pyroclastic fall deposits of So-OT are observed at 6 points on land. The most northern point is located in the southern Fukushima City. We newly defined Sawada fall pumice deposit (SwdP) at Tsurugaike in Shimogo Town, Fukushima. SwdP is sandwiched between lower APms and upper So-OT, and distribution and layer thickness are similar to So-OT fall tephra. SwdP has maximum refractive index of orthopyroxene similar to So-OT.

Stratigraphy of the pyroclastic flow deposits shown above and other tephras in descending order is So-OT, So-KT1, A<sub>2</sub>Pm (Suzuki & Hayakawa, 1990), So-KT2 and A<sub>1</sub>Pm (380-410 ka; Suzuki and Hayakawa, 1990; Suzuki, 2000; Machida & Arai, 2003), and BT72 (349 ka; Yoshikawa & Inouchi, 1991; Nagahashi et al., 2004) is positioned under So-KT1. A<sub>2</sub>Pm is positioned under Kkt (334 ka; Machida & Arai, 2003; Nagahashi et al., 2004)(Suzuki & Hayatsu, 1991). Correlation of A<sub>1</sub>Pm and A<sub>2</sub>Pm is confirmed by mineral composition and refractive index of orthopyroxene. These stratigraphical relationships indicate that ages of So-OT and So-KT1 is 300-349 ka and that of So-KT2 to be 334-410 ka.

Source of pyroclastic flow deposits and the eruptive history of Takahara volcano It is assumed the source of So-OT, So-KT1 and So-KT2 is the Shiobara caldera due to grain size of essential products in pyroclastic flow deposits, and distribution, grain size and thickness changes of fall deposits. From the results shown above and previous studies (Inoue et al., 1994; Okuno et al., 1997; Tsurumaki et al., 2013 etc.), we considered the eruptive history of Takahara volcano, and concluded

that it is roughly divided into 5 stages. Eruptions of the three pyroclastic flows equivalent to the second stage is Formation of caldera had occurred, within 100,000 years.

Keywords: Pyroclastic flow deposit, Takahara volcano, Shiobara Otawara tephra, Middle Pleistocene, Tephrochronology,

## Eruptions during 6000 years at Nikko-shirane volcano, Central Japan

\*Yuki Kusano<sup>1</sup>, Yoshihiro Ishizuka<sup>1</sup>, Teruki Oikawa<sup>1</sup>

### 1. Geological Survey of Japan

Six tephra layers are recognized in the Nikko-shirane volcano, central Japan without 1872-73 and 1889-90 AD eruptions. The top tephra layer at the foot of Mt. Nikko-shirane (Nks-1) is considered to be produced by 1649 AD eruption, which is the biggest one of the record. We show geology, petrography and radioactive carbon dating of these tephra at summit and foot of the Mt.

Nikko-shirane, and discuss about the volcanic history in the last 6000 years. Mode compositions of tephra 250-500  $\mu\text{m}$  in diameter were analyzed after washed out and separated into 250, 250-500, 500-1000 and >1000  $\mu\text{m}$  particles by wet sieve.

At the foot of Mt. Nikko-shirane, four tephra layers from the Nikko-shirane volcano and three alien tephra layers were recognized. The Nikko-shirane tephra layers are named Nks-1, 2, 3, 4 downward (Okuno, 1993). We subdivide the Nks-1 tephra deposit into Nks-1a, 1b, 1c, 1d downward based on the color and grain size differences at the sampling point. The Nks-1a-d tephra contain vesicular and transparent-light-colored glass (pumice), non-vesicular and light-colored glass, non-vesicular and dark-colored glass, lithic clast, altered clast, and plagioclase, quartz, clinopyroxene and orthopyroxene crystals. The Nks-1a-c also contain a small amount of vesicular and dark-colored glass (scoria). The Nks-1 tephra deposit contains 16% pumice in maximum.

Two of three alien tephra layers are the Asama-B and Haruna-ikaho tephra deposits downward, and both are intercalated between the Nks-1 and 2 (Okuno, 1993; Tsutsui et al., 2005). We found an alien tephra layer just beneath the Nks-3 tephra. It is brownish silty ash with altered orangey pumice at the sampling point. The tephra contains 15% vesicular and colorless glass and they have similar major element composition to the Asama-D tephra.

At the summit of Mt. Nikko-shirane, we found a 0.17 m thick tephra layer beneath 0.07 m thick surface soil. Lower part of the tephra shows grayish white and the upper part shows yellowish brown ash. More than 80% components of the tephra are lithic clast, altered clast, and colorless minerals. Radioactive carbon dating of black soil beneath the tephra indicates 1686-1731 and 1808-1927 cal AD (<sup>14</sup>C dating: 110  $\pm$ 20 yrBP). Based on the <sup>14</sup>C dating, the tephra layer would be produced by 1872-73 or 1889-90 eruption.

We propose that the Nks-1 might be magmatic eruption due to the Nks-1 tephra deposit contains 16% pumice in maximum. On the other hand, the tephra at the summit of Mt. Nikko-shirane should be the product of a phreatic eruption because of absence of pumice or scoria.

Keywords: Nikko-shirane volcano, Tephra stratigraphy, Holocene

## Historical eruption of Nikko Shirane Volcano

\*Teruki Oikawa<sup>1</sup>

1. Institute of Earthquake and Volcano Geology, Geological Survey of Japan, National Institute of Advanced Industrial Science and Technology

It summarizes the eruptive history of Nikko Shirane volcano on the basis of the historical records. The historical eruption of Niko Shirane Volcano was occurred at 1649, 1872-73, 1889-90 from historical records. All, after the fumarolic or rumbling activity, phreatic eruption has occurred. In addition, lahars occurred. Lahars were generated by overflowing water (hot springs) from the crater with the eruptions.

Keywords: Nikko Shirane, eruption, historical record, lahar, phreatic eruption

Two eruptive events occurred around 40 ka at the Akagi volcano in North Kanto, NE Japan:  
Eruptions of the Akagi-Kanuma and Akagi-Shimizu Lithic Tephra

\*Shohei Nanri<sup>1</sup>, Takehiko Suzuki<sup>1</sup>

1. Faculty of Urban Environmental Sciences, Tokyo Metropolitan University

Mt. Akagi, located in the northern Kanto, Northeast Japan, is a large Quaternary stratovolcano. The Mizunuma Chert Lapilli Pumice (CLP) dominated by accidental lithic fragments had been reported by Moriya (1968). The aim of this study is to clarify (i) distribution, (ii) stratigraphic position, (iii) sedimentary structure, (iv) petrological features, (v) mineralogical features, (vi) volume and (vii) eruption style, for CLP in more detail. We found new features of CLP then, the deposit was re-defined as the "Akagi Shimizu Lithic Tephra (Ag-SLT)". The Ag-SLT is distributed to eastern region from Mt. Akagi. The Ag-SLT exists on the Akagi Kanuma Pumice (Ag-KP), erupted at 44 ka. The Ag-SLT is composed of four units: 1L, 2P, 3P, 4L, with lithic fragments from Ashio Belt. Unit 1L has accretionary lapilli ( $\phi 13$  mm) in its bottom layer. The yellow pumice clasts within the unit 2P has high SiO<sub>2</sub> (77.5 - 80.0 wt.% : in major elements chemical composition in volcanic glass), compared to that in Ag-KP (76.0 - 77.5 wt.%). Unit 3P is Plinian deposits with pumice and lapilli. Unit 4L is Phreatomagmatic eruption deposits. The Volume of Ag-SLT is about 6 km<sup>3</sup> (VEI=5) as the same as the Hoei eruption of Mt. Fuji in 1707. The pumice within the Ag-SLT was formed with crystallization differentiation in magma reservoir. The interval of eruptions (dormant period) was suggested by the existence of the volcanic soil deposits (Tephric loess, so-called Loam) between Ag-KP and Ag-SLT.

Keywords: Mt. Akagi, Plinian eruption, lithic tephra, Ag-KP, Ag-SLT

## Holocene eruption history of the Motoshirane Pyroclastic Cone Group, Kusatsu-Shirane Volcano

\*Aki Nigorikawa, Yasuo Ishizaki<sup>1</sup>, Nobuko Kametani<sup>2</sup>, Mitsuhiro Yoshimoto<sup>3</sup>, Akihiko Terada<sup>4</sup>, Kenta Ueki<sup>5</sup>, Kentaro Nakamura<sup>6</sup>

1.Graduate School of Science and Engineering, University of Toyama , 2.Graduate School of Science and Engineering for Education, University of Toyama , 3.Mount Fuji Research Institute, Yamanashi Prefectural Government, 4.Volcanic Fluid Research Center, Tokyo Institute of Technology, 5.Japan Agency for Marine-Earth Science and Technology, Department of Solid Earth Geochemistry, 6.Paleo Labo Co.,Ltd.

The Kusatsu-Shirane Volcano, one of the most active volcanoes in Japan, is situated near the boundary of the Gunma and Nagano Prefectures. The summit of the volcano consists of three young pyroclastic cones, i.e., the Motoshirane Pyroclastic Cone Group (MPCG), the Ainomine Pyroclastic Cone, and the Shirane Pyroclastic Cone Group (SPCG). All historical (phreatic) eruptions occurred in the summit area of the SPCG. In contrast, the eruptive history of the MPCG has not yet been studied in detail. In order to decipher the eruption history of the MPCG, correlations between eruptives constituting the pyroclastic cone edifices and dispersed tephra are investigated. Petrological affinities, such as whole rock major-element chemistry and mineral assemblages, are utilized to identify eruptives contemporaneous with various modes of emplacement. The MPCG consists of a group of overlapping pyroclastic cones, including Kagamiike-kita, Kagamiike, Younger Motoshirane, and Older Motoshirane, which are arranged from north to south. The summit of each cone is cut by overlapping craters. In addition, three lava flows, i.e., the Isidu, Sessho, and Furikozawa lavas, poured out from the bases of the Younger Motoshirane, Kagamiike, and Kagamiike-kita cones, respectively. Stratigraphic relations suggest that each cone consists of three eruption stages; the initial lava-flowing stage, the subsequent cone-forming stage (accompanied by dome extrusion), and the final crater-enlarging explosion stage. The surface of the Older Motoshirane cone is covered by a bomb layer, which formed during the crater-enlarging stage of the adjacent Younger Motoshirane cone. In turn, the surface of the Younger Motoshirane cone is covered by the bomb layer that formed during the crater-enlarging stage of the adjacent Kagamiike cone. The proximal eruption products of the Kagamiike cone can be correlated with the 12L Volcanic Sand (4.9 cal ka BP; Yoshimoto et al., 2013) on the eastern foot based on geochemical affinities. We identified six new phreatic tephra layers sandwiched by soil layers on the southern flank of the Kagamiike cone. Here, the volcanic bombs from the Kagamiike-kita cone (probably formed during the crater-enlarging stage of the Kagamiike-kita cone) rest on the brown soil of ca.1.5 cal ka BP. In summary, the volcanic activity of the MPCG sifted from south (Older Motoshirane cone) to north (Kagamiike-kita cone), lasting until ca. 1,500 yr. BP. This study was supported by a grand-in-aid for young scientists from PaleoLabo Co. Ltd.

Keywords: Kusatsu-Shirane Volcano, Holocene, eruption history

## Clues to Reconstruction of Sequence of Eruptions in the Early Stage of the Asama-Maekake Volcano

\*Maya Yasui<sup>1</sup>

1.College of Humanities and Sciences, Nihon University

The Asama-Maekake volcano has been active for about 10,000 years. Little information, such as the distribution and stratigraphy of the eruptive products including pyroclastic fall deposits, pyroclastic flow deposits, and lava flows, is available for eruptions predating the 12<sup>th</sup> century owing to the lack of outcrops, especially in the proximal area. However, many pyroclastic fall deposits have been recognized in the distal area, mainly in the southeast direction, in previous studies, indicating that large-scale eruptions occurred repeatedly in the history of the volcano. In this study, the distribution of a pyroclastic fall deposit called Miyota pumice (referred to as As-My hereafter), which is distributed south of the summit crater, was mapped. The C14 ages of the samples of black humus soil that is covered with As-My, were dated to ca. 6400 cal.YBP. These ages are almost the same as that of the pyroclastic fall deposit As-UB distributed on the northern flank. The As-UB contains many fall units and is associated with a small-scale pyroclastic flow deposit in the proximal area. Bulk-rock chemical compositions of the pumice grains from As-My and As-UB were plotted in similar area to those for As-E on a SiO<sub>2</sub>-MgO variation diagram. These data suggest that the As-My, As-UB, and As-E are products from eruptions that occurred around 6000 years ago or a single eruption. Although the stratigraphic relation among these deposits distributed in different directions is difficult to determine, the fragmental information described above is expected to be helpful for reconstructing the sequence of eruptions in the early stage of this volcano.

Keywords: Pyroclastic fall deposit, stratigraphy, Asama-Maekake Volcano



What happened during the climactic stage of Tenmei eruption of Asama-Maekake volcano in 1783AD?: detailed process of the eruption of Agatsuma pyroclastic flow and Onioshidashi lava flow.

\*Masaki Takahashi<sup>1</sup>, Maya YASUI<sup>1</sup>

1.Department of Erath and Environmental Sciences, College of Humanities and Sciences, Nihon University

The detailed process of eruptions of Agatsuma pyroclastic flow and Onioshidashi lava flow during the climactic stage of Tenmei eruption (1783AD) of Asama-Maekake volcano is reexamined, based on the occurrence of volcanic deposits, their stratigraphy and old documents. The Agatsuma pyroclastic flow deposit comprises four stages: the earliest, early, A-scoria flow and late stages. The pyroclastic flows of the earliest stage and A scoria flow were the column-collapsed type. Those of the early stage were the boilover type and those of late stage were the fountain-collapse type. The Onioshidashi lava flow is clastogenic and consists of three units: L1, L2 and L3. The L1 and L3 are the slope-collapsed (rootless) type; the formation of L1 was synchronous with the last stage of Tenmei pumice fall deposits (21p), which were the climactic sub-Plinian eruption. The L2 is the spatter-fed type, outpouring from the crater of Kamayama welded pyroclastic cone. The earliest stage of Agatsuma pyroclastic flow was small-scale and occurred during the eruption of Tenmei pumice fall deposit around 18:00 in August 3 (corresponding to 10a to 14a). The early stage of Agatsuma pyroclastic flow began during the dormant stage of eruption of Tenmei pumice fall deposit from 16:00 to 18:00 in August 4 (corresponding to 20a). The pyroclastic flow deposits of the early stage with low aspect ratio are abundant in matrix ash, the essential clasts of which are high in SiO<sub>2</sub> (62 to 64wt. %). The A-scoria flow was small-scale and erupted during the eruption of Tenmei pumice fall deposit around 20:00 and 24:00 in August 4. The late stage of Agatsuma pyroclastic flow deposit erupted from 3:00 to 6:00 in August 5 just after the cessation of Tenmei pumice fall deposit. They show high aspect ratio and are relatively poor in matrix ash, the essential clasts of which are low in SiO<sub>2</sub> (61 to 62wt. %). The L1 of Onioshidashi lava flow with relatively high SiO<sub>2</sub> content (60.5 to 64wt. %) began to flow down around 18:00 in August 4 during the eruption of Tenmei pumice fall deposit and continued to 3:00 in August 5. The onset of effusion of L2 with relatively low SiO<sub>2</sub> content (60 to 63wt. %) was around 3:00 in August 5 concurrent with the eruption of late stage of Agatsuma pyroclastic flow. The flowing down of L3 (60.5 to 61.5wt. %) of the Onioshidashi lava formed by the collapse of slope of Kamayama pyroclastic cone was later than 3:00 in August 5.

Keywords: Asama volcano, Tenmei eruption, pyroclastic flow, clastogenic lava flow

Lava tubes and lava tube caves are formed in the lava flow of Nishinoshima volcano in Ogasawara islands?

\*Tsutomu Honda<sup>1</sup>

### 1. Vulcano-speleological Society

[Introduction] Nishinoshima which consists of andesite lava continues an eruption since November 20, 2013. Various reports<sup>1),2)</sup> on the previous 1973 year eruption and on this 2013 eruption are referring about existence of "lava tunnel" (lava tube or lava tube cave). Here, the possible formation of "lava tunnel" was considered based on hydrodynamic model as Bingham fluid. Because a lava tube cave (lava tunnel) exists clearly in a basalt lava flow, however, any lava tube caves have not been found hitherto in an andesite lava flow<sup>3),4)</sup>.

[Hydrodynamic model of a lava tube and hollow (lava tube cave) formation] A considered model is indicated on figure 1 where  $M$  is head height by magma pressure,  $L$  is length of lava tube and  $R$  are the lava tube radius, and  $\alpha$  is slope angle of a lava tube. Case(A) shows the lava spouted from a crater goes down a slope and forms a lava tube. The flow in the lava tube is controlled by the magma pressure and gravity (forced flow). After the termination of eruption, two cases (B) and (C) are considered. Case(B) shows a "filled lava tube" in which lava is stayed in the tube without drained out from the tube. Case (C) shows a "lava tube cave" in which the lava in the tube can be drained out by the gravity (free flow), a hollow is formed in the tube. For Case (A),  $M/L > 0$  and  $\tau_w = (\rho g \sin \alpha + \rho g M/L) R/2 > f_b$ , for Case(B), or Case(B),  $M/L = 0$  and  $\tau_w = (\rho g \sin \alpha) R/2B$ , for Case(C),  $M/L = 0$  and  $\tau_w = (\rho g \sin \alpha) R/2 > f_b$ , where  $\tau_w$  is shear stress on the tube wall,  $f_b$  is Bingham yield strength of lava,  $g$  is the gravity force and  $\rho$  is lava density.

[Estimate of a presence of a lava tube and a lava tube cave] From the correlation line between  $\text{SiO}_2$  wt% and Bingham yield strength of Hulme<sup>5)</sup>, the Bingham yield strength for 58~60 % is  $5 \times 10^4 \sim 10^5$  N/m<sup>2</sup>. The slope angle of lava flow is estimated as 6 degree from "Cross section of Nishinoshima for 2013.12.4.~2015.7.28" of Japanese Geological Survey. The estimated limiting lava tube height ( $H=2R$ ) calculated for  $M/L = 1.0$  and  $0.5$  and also  $M/L = 0$  is shown in table 1. In case of  $M/L = 0$ , the formation of a lava tube cave is impossible. On the other hand, in case of  $M/L > 0$  where pressurization by a magma is existing in the tube, there is a possibility of the lava tube formation depending on lava flow thickness. The followings are summary from the estimation based on the model:

- (1) The magma pressure enough to overcome the high Bingham yield strength of andesite lava should be acting in the lava tube to make flow the lava in a lava tube.
- (2) Even if a lava tube is formed, and when magma pressure is deleted, the lava will not be drained out from the lava tube. Then, lava tube cave will not be formed, only filled lava tube will be found.

[Conclusions] For the Nishinoshima lava flow of andesite, a lava tube cave will not be able to be found. Instead, there is a possibility to find a filled lava tube. The inspection of the lava flow thickness, the lava tube length/the height, the degree of the slope in Nishinoshima after landing is expected<sup>6)</sup>. A clear definition as a technical term of the lava tunnel or the lava tube is necessary. Use of active lava tube, filled(plugged) lava tube and drained lava tube(lava tube cave) is proposed.

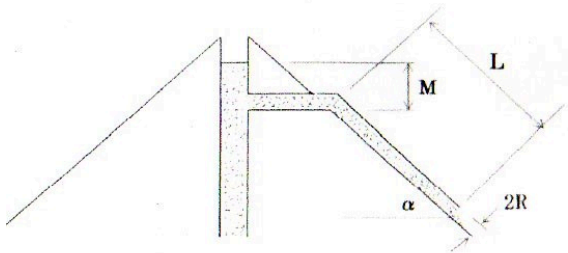
[References]

- 1) H. Aoki, J. Osaka (1974): Kaitaikazan no Nazo, p66, Tokai Univ. Press
- 2) T. Morishita, et al (2015): 2015 Fall Meeting of Volcanol. Soc. Japan, P85, p183

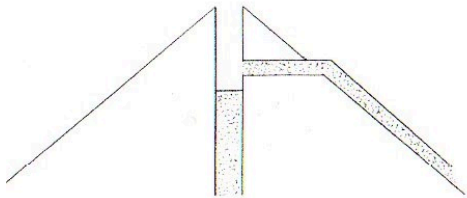
- 3)I.Moriya(1983):Nihon no kazanchikei ,p9,Tokyo Univ.Press
- 4)T.Honda,J.C.Tinsley(2015):2015 Fall Meeting of Volcanol.Soc.Japan, B3-03,p79
- 5)G.Hulme(1974):Geophys.J.R.Astr.Soc.,vol39,p361
- 6)T.Honda(2015):Caving Journal,No.53,2015.4,p24

Keywords: Lava tube cave, Nishinoshima, Andesite lava flow

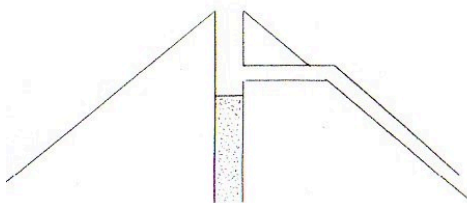
Fig.1 Hydrodynamic Model of Bingham Fluid



(A) Active lava tube:  $(\rho g \sin\alpha + \rho g M/L)R/2 > f_B$



(B) Filled lava tube:  $(\rho g \sin\alpha)R/2 < f_B$



(C) Drained lava tube:  $(\rho g \sin\alpha)R/2 > f_B$

Table1 SiO<sub>2</sub>wt% and Lava tube/cave height(Slope angle=6°)

SiO <sub>2</sub> wt%, Yield strength	Acting pressure : M/L=	Required tube height:H	Comparison with lava thickness:h(<50m)
SiO <sub>2</sub> 58%: *5x10 <sup>4</sup> N/m <sup>2</sup>	1.0 (Magna+Gravity)	7m	<h?(Tube formation?)
	0.5 (Magna+Gravity)	13m	<h?(Tube formation?)
	0 (Gravity)	80m	>h(No cave formation)
SiO <sub>2</sub> 61%: *1x10 <sup>5</sup> N/m <sup>2</sup>	1.0 (Magna+Gravity)	15m	<h?(Tube formation?)
	0.5 (Magna+Gravity)	26m	<h?(Tube formation?)
	0 (Gravity)	120m	>h(No cave formation)

\*G.Hulme(1974):Geophys.J.R.Astr.Soc.,vol39,p361

## Restudy of the eruptive history on Daisen Volcano, SW Japan

\*Takahiro Yamamoto<sup>1</sup>

### 1. Geological Survey of Japan, AIST

Daisen is a Quaternary volcano situated in SW Japan, and consists of adakite lava domes, pyroclastic flows and Plinian fall deposits. Although the eruptive history of this volcano has revealed by Tsukui (1984), the large frames of the history do not reach the quantification. Particularly, ca. 50-ka Daisen-Kurayoshi eruption which was the largest Plinian-type one, but was not understood whether this eruption was the thing which got up in the long-term volcanic activity of this volcano how. Therefore, this study performed revision of the stratigraphy of the past approximately 200,000 years of this volcano, radiocarbon dating and a re-measurement of the magma discharge quantity. In the point that is important by the revised stratigraphy, the Misen pyroclastic flow of Tsukui (1984) is divided into the Shimizuhara pyroclastic flow derived from the Sankoho lava dome in the north foot and the Masumizuhara pyroclastic flow derived from the Misen lava dome in the west - southwest foot; their essential materials differ in chemical compositions. The new radiocarbon calendar ages are 18,960-18,740 calBC and 26,570-26,280 calBC for the former and latter, respectively. Therefore, the youngest eruption was the formation of the Sankoho lava dome in approximately 20,000 years ago. Furthermore, this study rewrote the isopach maps for the tephra layers of this volcano origin and measured quantity of tephra volumes by the Legros (2000) method again. The tephra which quantity of volume came to largely have a bigger than a value conventionally is the ca. 80-ka Daisen-Namateke eruption, and its the smallest volume is 2 km<sup>3</sup>DRE. The revised magma discharge rate shows that a high state continued in this volcano for approximately 100,000 years, and the Daisen-Kurayoshi eruption is not specifically big in activity at this time of Daisen Volcano.

Keywords: Daisen Volcano, eruptive history

## Direction of natural remanent magnetization of rhyolite lava with clearly marked flow structure

\*Koji Uno<sup>1</sup>, Kuniyuki Furukawa<sup>2</sup>, Yoko Kaneshige<sup>3</sup>

1.Graduate School of Education, Okayama University, 2.Faculty of Business Administration, Aichi University, 3.Faculty of Education, Okayama University

Volcanic rocks have long been recognized as good recorders of the geomagnetic field corresponding to the time of their formation. Rhyolite lava is a common volcanic rock in continental regions and can also be considered to be a useful source of paleomagnetic data. However, only few studies have focused on paleosecular variation, magnetostratigraphy or plate reconstruction analysis using the remanent magnetization of rhyolite lavas. Being highly viscous, rhyolite lavas often show heterogeneous texture, unlike andesitic and basaltic lavas. Flow structure, one of the characteristics of rhyolite lava, may offer a clue about the changes in the direction of remanent magnetization in rhyolite lava during the development of the structure: heterogeneous texture in rocks may cause the deflection of the remanent magnetization to a direction different from the original one. The disagreement between the observed paleomagnetic direction of rhyolite lava and the expected one may be a function of the development of the flow structure.

In this study, we examined a thick rhyolite lava flow with clearly marked flow structure to assess its ability to records a consistent paleomagnetic direction, using material penetrated by two drill cores.

Progressive thermal demagnetization isolated two natural remanent magnetization components. The remanence was almost unblocked at around 580 degrees C during thermal demagnetization and is inferred to be carried by magnetite. A high-temperature component from each of the two cores yields inclinations that differ from each other. The low-temperature component had those that agreed with each other, and were also consistent with the direction expected from a geocentric axial dipole field. The modification of direction of the high-temperature component may be explained by post-magnetization acquisition tilting. In the case of silicic lava, the low-temperature component may retain directions parallel to the ambient field direction at the time of lava emplacement.

Keywords: Rhyolite lava, Remanent magnetization, Drill cores

## Petrological characteristics of Aso-ABCD tephra which erupted before Aso-4 pyroclastic eruption

Fumiko Sugiyama<sup>1</sup>, \*Toshiaki Hasenaka<sup>1</sup>, Atsushi Yasuda<sup>2</sup>, Natsumi Hokanishi<sup>2</sup>, Yasushi Mori<sup>3</sup>

1.Graduate School of Science and Technology, Kumamoto University, 2.Earthquake Research Institute, University of Tokyo, 3.Kitakyushu Museum of Natural History and Human History

Several tephra layers such as Aso-A, B, C, D, , , M, N,  $\alpha$ ,  $\beta$ , , ,  $\eta$ , between Aso-4 (89 ka) and Aso-3 (123 ka) pyroclastic eruptions have been described by Ono et al. (1977). Among them, Aso-ABCD is located at the top of all, and represent a series of continuous eruption events. Nagahashi et al. (2007) estimated their age as 97.7 ka. Ono et al. (1977) estimated the eruption source to be the south of present central cones from the isopach maps. Machida and Arai (1992) estimated their volume to be 3.5 km<sup>3</sup>. Just before the eruption of Aso-4 event occurred the formation of Omine pyroclastic cone and associated Takayubarū lava flow. This lava flow is overlain by Aso-4 tephra with no intercalated soil. The volume estimate is 2 km<sup>3</sup>. The most voluminous felsic eruption after Aso-4 event was that of Kusasenri-ga-hama volcano with 1.4 km<sup>3</sup> volume (Miyabuchi, 2003). Thus, Aso-ABCD and Omine volcanoes represent voluminous precursory eruptions before caldera-forming Aso-4.

Pumice and volcanic ash was sampled 20 km east of Aso caldera, where the thickness of Aso-ABCD tephra in total is 3 m. The samples were analyzed for XRF bulk-rock chemical analysis, EPMA mineral analyses, FT-IR analyses of melt inclusions. Phenocryst assemblage is plagioclase, clinopyroxene, orthopyroxene, and magnetite, with no hornblende which is common in Aso-4 products. Bulk composition of pumice ranges 63-66 wt. % silica, and mostly plot on Aso-3 trend, and not on Aso-4 trend of Kaneko et al. (2007, 2015). Melt inclusions in plagioclase and pyroxenes also show compositions similar to glass of Aso-3 with silica range mostly in 70-72 wt. %. Compositional range of phenocryst cores are An<sub>40-64</sub> for plagioclase, Mg# =70-74 for orthopyroxene, and Mg#=74-81 for clinopyroxene. Water content was estimated to be 1.0-4.8 wt.% for melt inclusions in host minerals of An<sub>40-64</sub> plagioclase, Mg#=70-74 orthopyroxene, and Mg#=74-81 clinopyroxene.

Equilibrium relationship between melt inclusion and host clinopyroxene provides temperature estimate of 860-950 °C and pressure estimate of 1.1-2.7 kbar (Putirka, 2008). The pressure corresponds to the depth of 3-9 km, comparable to the estimated depth (6 km) of present Kusasenri-ga-hama magma reservoir. Furukawa et al. (2006) showed a gradual change of tephra composition, estimated temperature, estimated water content, and estimated oxygen fugacity from Aso-3 to Aso-4. However, our study showed similarity of magma composition between Aso-ABCD tephra and Aso-3 products. Aso-4 magma reservoir was not yet prepared 9000 years before Aso-4 eruption. Or Aso-4 reservoir at that time was independent from, and had no interaction with, other magma supply system then.

Keywords: Aso, caldera-forming eruption, melt inclusion, Aso-ABCD tephra, Aso-4 pyroclastic eruption

CSD (Crystal Size Distribution) analysis for plagioclase phenocrysts in historical lavas of Sakurajima volcano -The control of magma plumbing system for the eruptive style and frequency-

\*Shunsuke Yamashita<sup>1</sup>, Atsushi Toramaru<sup>2</sup>

1.Department of Earth and Planetary Sciences, Graduate School of Science, Kyushu University,

2.Department of Earth and Planetary Sciences, Faculty of Science, Kyushu University

In order to obtain insights into roles played by magma plumbing system in the long-term behavior of eruptive activity, we conducted crystal size distribution (CSD) analysis of plagioclase phenocrysts in four historical lavas of Sakurajima volcano, located in southern Kyushu, Japan: Bunmei eruption (1471-76), An-ei eruption (1779-82), Taisho eruption (1914-15), and Showa eruption (1946). Bunmei, An-ei, and Taisho eruptions firstly fell pumice by Plinian eruptions from newly formed flank vents, and subsequently flowed lavas. Showa eruption firstly had fell ash frequently for about three months, and subsequently flow lava from the Showa crater. After Showa eruption, Vulcanian eruptions occurred frequently, indicating the temporal change of eruptive style from large volume Plinian eruptions with lava flows (c.a. 1 km<sup>3</sup> DRE) to small volume frequent eruptions (one event less than 10<sup>-3</sup> km<sup>3</sup>).

In four historical lavas, plagioclase phenocrysts are classified into 3 types. Type-A is represented by the clear texture and lower An content (around An<sub>60</sub>) in core and rim. Type-B shows the clear texture and higher An content (around An<sub>80</sub>) in core and lower An content (around An<sub>60</sub>) in rim, and the sharp compositional contrast between the core and the rim. In addition, the length of rim varies by a wide range as 10-200μm in all lavas. Type-C has the sieve texture and heterogeneous compositions in core. From above chemical analysis, the magma plumbing system consist of two magma reservoirs (felsic magma chamber and mafic magma chamber) where the crystallization proceeds to form phenocrysts. Type-A crystallizes in the felsic magma chamber in which the compositions gradually changes from felsic to mafic during hundreds years by repeated injections of mafic magmas. Type-B crystalizes in the mafic magma chamber, and the mafic magma continuously injects to the felsic magma chamber.

The CSD plots of both type-A and type-B can be approximated by log-linear CSDs. Slopes of type-A are constant regardless of eruptive ages, and those of type-B become steeper with time, that is, Showa has the steepest slope. From the CSD analysis, the residence time in the felsic magma chamber is nearly constant with time, whereas the residence time in the mafic magma chamber becomes shorter with time, indicating that both mantle-derived mafic magma supply rate and extraction-rate to the felsic magma chamber increase with time. The magmatic behavior such as crystallization and accumulation rates in the felsic magma chamber keeps a constant pace and has no influence on eruptive phenomena. On the other hand, the mafic magma chamber located at deeper level controls the surficial behavior in eruptive phenomena, such as frequency of eruptive events and dominant eruption styles of Vulcanian type, through increasing rates of mantle-derived mafic magma supply.

Keywords: Crystal size distribution, Plagioclase phenocryst, Magma plumbing system

Tsunamis generated by the 7.3 ka catastrophic eruption at Kikai caldera, Japan: constraints from tsunami traces around the Koseda coast, NE Yakushima, Japan

\*Fukashi Maeno<sup>1</sup>, Futoshi Nanayama<sup>2</sup>, Shojiro Nakagawa<sup>3</sup>, Hiroyuki Sasaki<sup>3</sup>, Masamichi Omote<sup>3</sup>, Nobuo Geshi<sup>2</sup>, Kazuaki Watanabe<sup>2</sup>, Hideto Naruo<sup>4</sup>, Tetsuo Kobayashi<sup>5</sup>

1.Earthquake Research Institute, University of Tokyo, 2.Geological Survey of Japan, AIST, 3.Yakushima Earth Science Club, 4.Takeokadai High School, 5.Kagoshima University

Timing and mechanism of volcanogenic tsunamis are important to constrain nature, processes, and hazards of volcanic eruptions in marine and lacustrine environments. In this presentation, we report the event deposits caused by pyroclastic flows and tsunamis during a catastrophic caldera-forming eruption at Kikai caldera, Japan, and discuss their origin. There are some hypotheses on the tsunami generation and propagation during the 7.3 ka eruption at Kikai caldera. Previous numerical simulations showed that huge tsunamis might hit Yakushima Island (e.g., Maeno et al., 2006), but so far no clear and convincing evidence has been found in this region. We investigated traces of the tsunamis caused by this eruption in the northeast of Yakushima Island, and found the deposits, originated from the pyroclastic flow and tsunami event at 7.3 ka, near the Onagawa river mouth at the Koseda coast. Our study includes reinterpretation of a previously studied outcrop (Moriwaki et al., 2006). The deposits at the Koseda coast consist of two major units and lie on a wave cut bench (WB-4) of ~8.4 m above sea level or more. The lower unit is a poorly sorted, ~30-cm gravel bed with sandy matrix, and the upper unit is a massive, 0.3-1-m thick pyroclastic flow deposit from the 7.3 ka eruption. A reworked deposit and a 1-2-m thick gravel bed cover the pyroclastic flow deposit. Based on the outcrop and trench surveys, the lower gravel bed is traceable at least 120 m toward inland and has a similar component to modern beach gravels distributed around the Onagawa river mouth. The matrix of the lower gravel bed also contains pumice clasts (up to a few cm in diameter) originated from the 7.3 ka eruption, as evidenced by glass chemical composition and fibrous texture. The grain-size of the matrix component decreases toward inland. The local observations of Holocene marine terrace distributed in the northeast of Yakushima suggest that the highest sea level phase (+9.7 m) occurred between 7.3 and 5 ka. Thus, we interpret that WB-4 emerged before 7.3 ka, the sea level at 7.3 ka was less than 8.4 m, and a transgression of 1-2-m continued after 7.3 ka. Based on our data and interpretation, we would conclude that gravel in the lower bed was transported from the river mouth to the top surface of WB-4 by a relatively high concentration, energetic current associated with a tsunami at 7.3 ka, and that the timing of the tsunami is constrained after the beginning of the 7.3 ka eruption and before or during the climactic phase that produced large-scale pyroclastic flows.

Keywords: volcanogenic tsunamis, pyroclastic flows, Kikai caldera, Koseda coast, Yakushima



## Role of thermal boundary layer on microlite crystallization: constraints from shear-deformation experiments

Chizen Komamiya<sup>1</sup>, \*Michihiko Nakamura<sup>1</sup>, Satoshi Okumura<sup>1</sup>

1.Division of Earth and Planetary Materials Science, Department of Earth Science, Graduate School of Science, Tohoku University

Microlite crystallization in ascending hydrous magmas has been widely believed to be driven by decompression and resulting liquidus temperature increase, because thermal conductivity of magma is low and cooling is less effective for magmas ascending at a common velocity in a conduit. In the thermal boundary layer along conduit walls, however, effect of thermal conduction is imposed on the undercooling produced by decompression, thus microlite nucleation is supposed to be enhanced. The conduit walls may work also as a site for heterogeneous nucleation. In order to evaluate the potential role of thermal boundary layer on the microlite crystallization in ascending magmas, we have investigated experimentally the effect of temperature gradients and shear flow on the textural evolution and crystallization kinetics of trachyandesitic melt using an image furnace. The shear deformation was applied by twisting two rods, fixed to the upper and lower shafts. The rods of alumina were used in Series1 experiments. In Series2 experiments, dacite lava was used for the upper rod. The starting materials were initially heated at a temperature higher than the liquidus temperature for 60-120 minutes, then once quenched and reheated at a run temperature below the liquidus. The difference between the initial heating temperature and the liquidus was defined as superheating,  $-DT$ . The difference between the run temperature and the liquidus temperature, was defined as supercooling,  $DT$ . The experiments were performed at different degrees of superheating ( $-DT = 33, 98$  and  $233^{\circ}\text{C}$ ), supercooling ( $DT < 138^{\circ}\text{C}$ ) and rotation rates ( $0, 0.08$  and  $0.8$  rpm). In Series 1, run products had high crystal fraction only at low superheating ( $33^{\circ}\text{C}$ ), in which minute relict crystals worked as a nucleation sites. At higher superheating experiments ( $98$  and  $233^{\circ}\text{C}$ ) and static experiments without shear, no crystal was observed in the central part of the run products. On the other hand, the run products of Series2 had high crystal fractions even at a high superheating ( $-DT = 233^{\circ}\text{C}$ ) when the shear rate was high ( $>10^{-1} \text{ s}^{-1}$ :  $0.8$  rpm). The difference between Series1 and Series2 can be summarized as follows. The surface of the rods, both alumina and dacite, induced heterogeneous nucleation of plagioclase. However, the crystals formed on the alumina rod surface were spherite-like, whereas those on the dacite rod surface had a shape similar to natural microlites. The nucleated plagioclase crystals were removed from the rod surfaces by shear flow only from the dacite surface in Series2. The plagioclase crystals were brought to the inside of the samples, resulting in high crystal number density and volume fraction.

Assuming a simple plug flow with conductive cooling from the walls, the thermal boundary layer with  $DT=20^{\circ}\text{C}$  can be formed from the conduit wall with a thickness of a few percentage of the conduit radius. The strain rate at which the crystal can be removed from the boundary layer, i.e.,  $10^{-1} \text{ s}^{-1}$ , is achieved near the conduit wall if the ascent rate of magma is higher than  $5.0 \times 10^{-2} \text{ m s}^{-1}$ . These rates were observed in some eruptions such as Mount St. Helens. Crystal number density of the eruptive materials may, therefore, include the crystals formed at the thermal boundary layer near the conduit wall as well as the crystals nucleated in the conduit center solely by decompression. The effect of thermal boundary layer crystallization should be considered for number density and morphology of microlites in volcanic rocks.

Keywords: microlite, undercooling, magma ascent

